Dissolved Mn(III) in Water Treatment Works: Prevalence and Significance

Karen L. Johnson[1*], Clare M. McCann[2], John-Luke Wilkinson[3], Matt Jones[4&5], Bradley M. Tebo[5], Martin West[6], Christine Elgy[7], Catherine E. Clarke[8] Claire Gowdy[9] and Karen A. Hudson-Edwards[10]

[1]Department of Engineering, Durham University, South Road, DH1 3LE

[2]School of Natural and Environmental Sciences, Newcastle University, Newcastle upon Tyne, NE1 7RU.

[3]AECOM, Newcastle upon Tyne, NE1 2HF.

[4] School of Environmental Science and Engineering, Pohang University of Science and Technology (POSTECH), 77 Cheongam-ro, Nam-gu, Pohang-si, Gyeoungsangbuk-do, 37673, Korea.

[5]Institute of Environmental Health, Oregon Health & Science University, Portland, OR 97239 USA

[6]Department of Geography, Durham University, South Road, DH1 3LE

[7]Facility of Environmental Nanoscience Analysis and Characterisation, Department of Geography Earth and Enviromental Sciences, Edgbaston, Birmingham, B15 2TT

[8] Department of Soil Science, Stellenbosch University, Private Bag X1, Matieland 7602, South Africa

[9]Northumbrian Water Group Ltd., Boldon House, Wheatlands Way, Pity Me, Durham, DH1 5FA

[10]Environment & Sustainability Institute and Camborne School of Mines, University of Exeter, Penryn, Cornwall, TR10 9DF

*Corresponding author: Karen Johnson (karen.johnson@durham.ac.uk)

Highlights

1. Mn(III) has been identified at all stages for the first time through a water treatment works.
2. Mn(III) can be produced in water treatment works where waters are in contact with organic rich sludges.
3. Knowledge of Mn(II)/(III) speciation within WTW could help the Water Industry to improve Mn removal within WTW.

Graphical Abstract

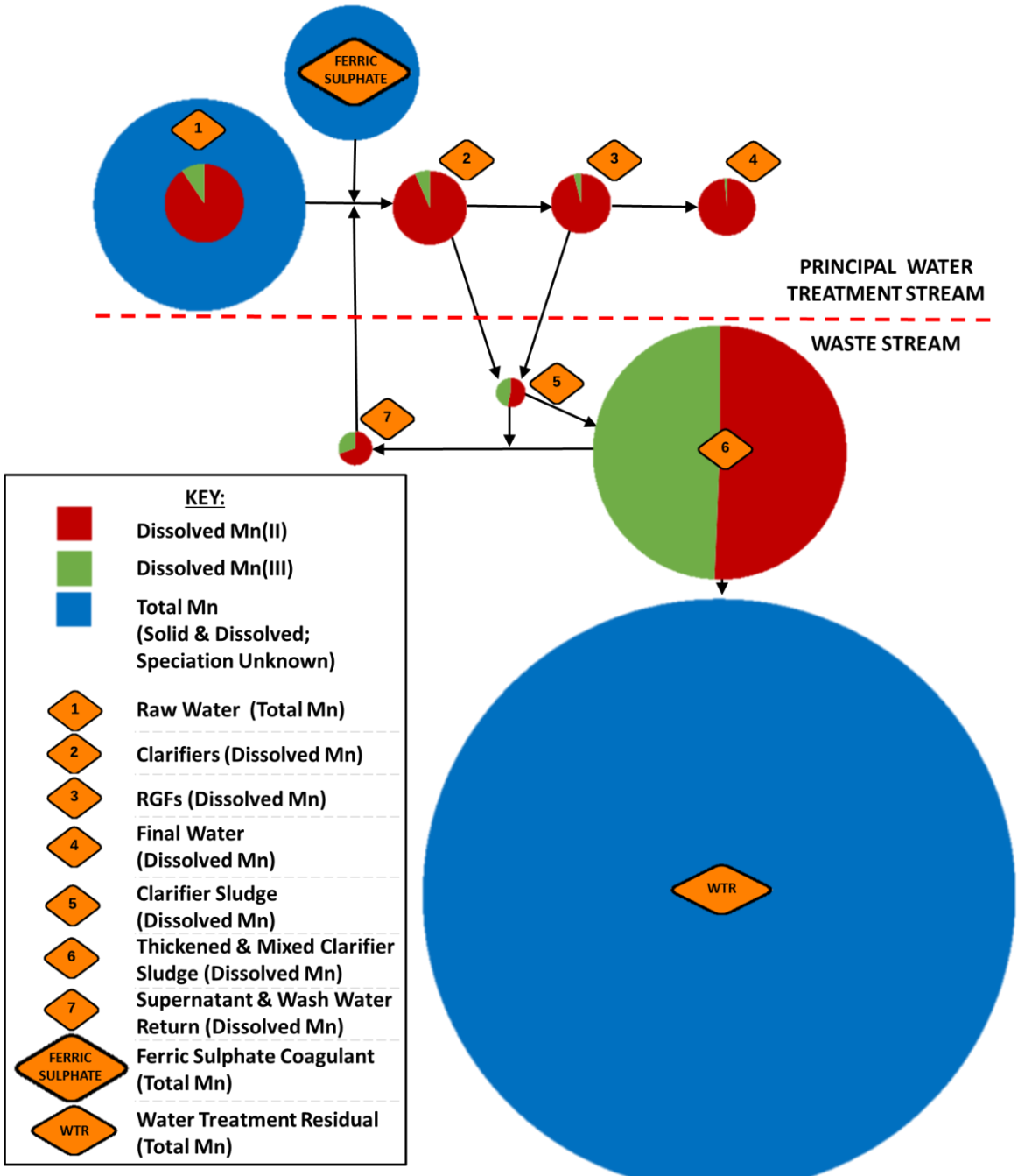

Abstract

Dissolved Mn(III) has been identified at all stages throughout a Water Treatment Works (WTW) receiving inflow from a peaty upland catchment in NE England. Ninety percent of the influent total manganese into the WTW is particulate Mn, in the form of Mn oxide (> 0.2 µm). Approximately 9 % (mean value, n = 22, range of 0 -100 %) of the dissolved (< 0.2 µm) influent Mn is present as dissolved Mn(III). Mn(III) concentrations are highest (mean of 49 % of total dissolved Mn; n = 26, range of 17 – 89 %) within the WTW where water comes into contact with the organic-rich sludges which are produced as waste products in the WTW. These Mn(III)-containing wastewaters are recirculated to the head of the works and constitute a large input of Mn(III) into the WTW. This is the first report of Mn(III) being identified in a WTW. The ability of Mn(III) to act as both an oxidant and a reductant is of interest to the water industry. Understanding the formation and removal of Mn(III) within may help reduce Mn oxide deposits in pipe networks. Further understanding how the ratio of Mn(III) to Mn(II) can be used to optimise dissolved Mn removal would save the water industry significant money in reducing discoloration 'events' at the customers' tap.

Key words: Manganese Removal, Water Treatment Works, Mn(III), Natural Organic Matter (NOM)

Abbreviations: WTW – Water Treatment Works; WTR – Water Treatment Residual; NOM – Natural Organic Matter; DOC – Dissolved Organic Carbon; RGF – Rapid Gravity Filters; NWG Ltd.– Northumbrian Water Group Ltd.

1 Introduction

Dissolved manganese (Mn) within water supplies has long been a problem for suppliers of potable water. Dissolved Mn is not generally regarded as toxic when ingested via oral routes (WHO 2011). Neurological effects of ingestion via inhalation of aerated waters high in Mn during showering are possible but it is generally agreed that the risk is low (Menezes-Filho et al. 2009). Due to this the World Health Organisation (WHO) have set guideline limits for Mn at the value at which it causes acceptability problems to consumers due to Mn(III)/Mn(IV) precipitates colouring the water (0.05 mg/L) which is below that of potential health effects (0.4 mg/L). Termed discolouration 'events' by the industry this can lead to staining of laundry for example (WHO 2011) which leads to customer dissatisfaction. Typically most Mn precipitates are removed during the normal processing procedure at the WTW (see section 1.1), but remaining dissolved Mn in water can lead to the build-up of Mn-fed microbial films in the network pipes depending on the final water pH and presence of residual oxidant. Sloughing of these build ups, caused by disturbances in the system — including pipe bursts, changes to flow patterns or the use of fire hydrants — can lead to sporadic re-suspension of precipitates, and hence colour, into the supply. Water companies are investing heavily in cleaning their network pipes in order to remove deposits of Mn and other metals (particularly iron), and hence the optimal extraction of metals within the WTW is perceived as critical to keep the network clean, (e.g. Johnston 2011). A better understanding of Mn speciation and distribution within the WTW is therefore required to help inform how dissolved Mn can be fully extracted before the water enters the network pipes. The differentiation between dissolved Mn(II) and Mn(III) in WTW is important as these species are likely to react differently throughout the water treatment process due to their differing chemical reactivities with both organic and inorganic species. Recent work by Hu et al. (2017)

has shown that unlike Mn(II), dissolved Mn(III) can take part in both oxidative and non-oxidative reactions with organic contaminants of relevance to the water industry.

1.1 Manganese removal in Water Treatment Works

Manganese is conventionally removed in the EU using aerated rapid gravity filter beds which utilise the 'greensand effect' whereby clean sand and anthracite become coated in Mn oxide layers to produce Mn-oxide coated sands which then autocatalyse Mn oxidation (Bruins et al. 2015). Particulate Mn (>0.45 μm) is removed in the first stage of the treatment process and Figure 1 shows this process step by step for a WTW in NE England (see section 2.1 for more details).

The coagulant ferric sulphate is added to screened water just before the raw water enters the clarifiers to encourage flocculation of suspended colloids. The resulting waste flocs are removed as a sludge and the wastewaters generated are recirculated to the head of the works for further Mn removal. The sludge is then taken from the site as a waste by-product. The water is also pH adjusted using lime to raise the pH, causing precipitation of dissolved Mn from the water as solid Mn oxides. This pH correction also takes place later in the process, before the water passes through the rapid gravity filters (RGFs) to maintain pH at 9.2 within the RGFs. Here dissolved Mn is adsorbed onto the RGF filter media and particulate material is filtered out of suspension. The RGFs are cleared, using a treated water backwash and air scouring to remove particulate material from the media, approximately every 60 hours, and the backwash water and material is passed into the waste stream. Consequently Mn is removed in both the clarifiers and in the RGFs. The waste sludges containing predominantly Fe and Mn oxides and natural organic matter (NOM), as well as other trace elements extracted in the process, are thickened and formed into a

semi-solid water treatment residual (WTR).

However, in the US, it is more common to use stronger oxidants such as potassium permanganate or sodium hypochlorite to remove manganese in water treatment works and manganese removal generally occurs at near neutral pHs. If permanganate or hypochlorite is added and there are humics present, the reaction would depend on how much dissolved Mn(II) and humics there are. If there is excess permanganate / sodium hypochlorite, then potentially all Mn(II) and NOM would be oxidised. Mn(III) will not be stable at near neutral pHs in the presence of Mn(VII) unless there is more Mn(II) than Mn (VII) present (Davies, 1969) or the organic ligand has not been oxidised. So if there is excess permanganate or a permanganate / sodium hypochlorite mix it is unlikely that the organic ligand is available to stabilise the Mn(III) (Yu et al. 2015). If there are Mn(III)-organic ligand complexes already in the system they will be oxidised by permanganate (Jiang et al. 2010) and this reaction appears to increase the oxidative capacity of the permanganate reactions towards contaminants. Sun et al. (2015) also show that even with a 60 micro-second life span of the Mn(III) ion (Davies 1969) there is an increase in the overall reaction rate of the oxidative removal of organic contaminants due to Mn(III)-organic ligands. This raises the possibility of the presence of Mn(III) – organic ligands in WTW potentially being a good thing although we present no evidence for this.

Manganese in natural waters

Manganese is prevalent in natural waters in temperate regions around the world and its release from soil is often correlated with dissolved organic carbon (DOC) concentrations with peaty soils often containing significant quantities of Mn (Hardie et al. 2007). It is known that Mn can

occur in peaty soil pore waters as nano-particulate Mn oxides (Krachler et al. 2012). Figure 2 shows the relations between Mn(II - dissolved), Mn(III – both dissolved and solid) and Mn(IV - solid) and soil organic carbon (SOC) which is present in peat. This study uses the operational definition of 'particulate' Mn as solids > 0.2 μm , and, 'dissolved' Mn as by what passes through a 0.2 μm filter. We focus on the speciation of the dissolved fraction.

Until recently it was thought that Mn occurred in solution as Mn(II) and in solid form as Mn(III) and Mn(IV) oxides (Tebo et al. 2004). In the last ten years, it has been determined that dissolved Mn(III) exists in numerous natural waters globally, after it was identified in suboxic sediment porewaters, stratified water bodies and most recently even in oxic marine waters albeit it at nano-molar concentrations (Trouwborst et al. 2006, Madison et al. 2011, Luther et al. 2015, Oldham et al. 2017, Oldham et al. 2015). Identification of Mn(III) within the largely oxic environment of a WTW is highly relevant to this body of work as it extends the reach of Mn(III) into oxic terrestrial waters. Identification of Mn(III) within WTW is also of great interest to the water industry to help them understand how best to improve Mn removal within WTW. This investigation investigates both the flux of Mn through the WTW as well as the speciation of the Mn present at each stage of treatment. Although there have been several studies examining the Mn(II)/Mn(III) speciation in anoxic marine pore waters (starting with Trouwburst et al, 2006) and more recently one study on the present of Mn(III) in oxic marine pore waters (eg Oldham et al 2017), there are no studies exploring Mn(II)/Mn(III)) speciation in any peaty terrestrial surface waters which naturally contain Natural Organic Matter (NOM). This paper aims to address this oversight and explore Mn speciation in peaty water which is influent to a water treatment works (WTW) and throughout the Mn removal process within the WTW. This is

important since high NOM content and the manganese cycle are intrinsically linked (e.g. Johnson et al 2015).

2 Materials and Methods

2.1 Field site – Mosswood WTW

Mosswood WTW is a Northumbrian Water Group Ltd. (NWG Ltd.) operated facility, located approximately 26 km from Durham in the North-East of England. The works are fed principally from Derwent reservoir, situated 3 km west of the site, although raw water can also be pumped, at significant cost, from Kielder reservoir or the River Tyne. The works are the largest operated by NWG Ltd., treating up to 145 ML of water per day, and supply the metropolitan areas of Sunderland and Durham. The work's operation can be split into three sub-streams as shown in Figure 1 above and described below.

2.1.1 Principal Water Treatment Stream

Raw water (pH 7.4) enters the plant and is collected from the upstream Derwent reservoir and surrounding peaty uplands (see Table 1 in Section 3). The raw influent water passes through debris screens, and is passed, via flash mixers to aerate the water and provide oxidising conditions, into the clarifiers. Lime and coagulant (ferric sulphate) are added at the flash mixer inlet to raise the pH (to pH 9.2) and promote flocculation of particulate material within the water. Once in the clarifiers, the water is slowed to allow settlement of the solid material, while the remaining water is drawn from the surface. The solid material is removed as a sludge into the solid waste removal stream. The water is then passed to the Rapid Gravity Filters (RGFs), with a further addition of lime to keep the pH above 9 and again promoting precipitation of dissolved

Mn. These filters are comprised of 1 m-deep manganese oxide-coated greensand and anthracite beds through which the water is allowed to percolate, with solid particles being trapped within the filter media, and dissolved Mn being adsorbed and then oxidised (by dissolved O_2) onto the greensand particles, forming layers of Mn oxides around the media particles (McCann et al. 2015). The filter media is cleaned every 60 hrs using an air scour and treated water backwash to dislodge and remove particulate material. The backwash water and dislodged particulate material is removed to the solid-waste removal stream. From the RGFs the water is chlorinated to inactivate pathogens harmful to humans, and then is discharged from the plant to storage facilities and finally to the consumers.

2.1.2 Solid Waste Removal Stream

The waste removed from the clarifiers and RGFs is passed through a separate solid waste stream as part of the plant waste removal. Sludge from the clarifiers is passed to settling tanks where the solid component of the sludge is allowed to settle and the supernatant above the sludge is drained to a separate holding tank. The settled sludge is passed onto another holding tank where it is mixed with a small quantity of polyelectrolyte (in this case starch) to promote thickening. Starch is added as a flocculant to help the Fe oxide precipitates in the waste sludge to coagulate and ultimately increase the density of these voluminous precipitates to reduce transport costs.

Finally this sludge is passed through a centrifuge to reduce the water content as much as possible to make the waste product Water Treatment Residual (WTR). At this WTW, the WTR is then spread on the land. However, for many other WTWs, WTR is a waste product which is often sent to landfill.

2.1.3 Liquid Waste Recycling Stream

158 The backwash from the RGFs and the supernatants from all of the various sludge tanks (clarifier,
159 mixed and thickened sludge) is extracted to yet another tank to allow for the settlement of any
160 further suspended material. The final supernatant is recycled to the head of the works, where it is
161 mixed with the raw water by way of the flash mixers after the lime and ferric sulphate but before
162 the addition of starch.

163 **2.2 Sampling**

164 Samples were collected over 12 days in 500 mL sterile bottles on a daily basis during a 2 month
165 period from seven locations within the plant in Winter 2014/15. Samples were taken by staff at
166 the works as part of their regular quality- assurance sampling regime (Figure 1) and the smallest
167 number of samples (labelled 'n' in Section 3.0) was 12 for the final water (sample point 7). Extra
168 samples were taken wherever possible so 'n' ranges from 12 to 26 depending on sample point.
169 Each 5-day batch of samples was collected from the works at the end of the working week and
170 brought back to the laboratory for processing. The samples were shaken to ensure reasonable
171 homogeneity and then 50 mL subsamples were filtered using syringe- mounted 0.2 μm
172 membrane filters. The samples were then stored at 4°C until required, although samples were
173 processed as quickly as possible following collection and filtration to minimise the chance of
174 possible bottle reactions. It was established that the holding time of 5 days at the works had
175 minimal effect on dissolved manganese as replicate samples taken at each stage and stored for
176 different times were within 8 % of one another (see Table S1 in Supplementary Material).

177 **2.3 Experimental Method**

178 ***2.3.1 Determination of Mn(III) and Mn(II)***

The experimental method used in this project was based on the method developed by Madison et al. (2011) and has a detection limit of 50 nM Mn(III). No replicates were carried out on each 50 mL subsample. All chemicals were reagent grade, and all solutions prepared with deionised water (DI) water. A 2×10^{-4} M solution of α,β,γ,δ-tetrakis(4-carboxyphenyl)porphine [T-(4-CP)P] was prepared by dissolving 0.2 g of crystalline T-(4-CP)P (Frontier Chemicals, CAS14609-54-2) in 3 mL acetone to purify it, drying overnight, and then dissolving 28.5 mg purified T-(4-CP)P in 2.5 mL 0.04 M NaOH and making up to 100 mL with DI water. Precautions to ensure low light levels were taken during both the preparation and use of the T-(4-CP)P solution due to its photosensitivity. A 900 μM cadmium chloride ($CdCl_2$) solution was prepared by dissolving 16.5 mg crystalline $CdCl_2$ in 100 mL DI water. A buffer solution was prepared using 50 mL of 0.025 M sodium tetraborate decahydrate, 20 mL of 0.1M hydrochloric acid and 25 mL of 0.6 M imidazole. This buffer solution was then pH adjusted to pH 8.0 using 3 M HCl, before being made up to 100 mL with DI water. Mn(II) standard solutions were prepared from a 0.01 M stock Mn solution from anhydrous Mn(II)chloride ($MnCl_2$) powder dissolved in 1 mL of 0.1 M HCl, made up to 100 mL with DI water.

2.3.1.1 Kinetic Scan Method

Luther et al. (2015) further developed the method utilising the T(4-CP)P complex, addressing the existence of Mn(III) as well as Mn(II) within the samples. Luther et al. (2015) found that both Mn(II) and Mn(III) can react with the Cd^{2+} T(4-CP)P complex to form the same end product via two separate reaction pathways (equations (1-3)):

$$Mn^{2+} + Cd^{2+}\cdot T(4-CP)P \xrightarrow{"Cd^{2+}} Mn^{2+}\cdot T(4-CP)P \quad (1)$$

$$Mn^{2+}\cdot T(4-CP)P + O_2 \longrightarrow Mn^{3+}\cdot T(4-CP)P \quad (2)$$

$$Mn^{3+} + Cd^{2+}\cdot T(4-CP)P \xrightarrow{"Cd^{2+}} Mn^{3+}\cdot T(4-CP)P \quad (3)$$

199

200 Since the Mn(III) transfer to form the Mn(III)T(4-CP)P complex takes place via ligand exchange
201 – removing the Mn(III) from the organic ligands holding it in solution – the rate of Mn(III)T(4-
202 CP)P formation from the Mn(III) ion is slower than from the Mn(II) ion (Luther et al. 2015). It is
203 therefore possible to model the metal-exchange reactions using a simple kinetic model, and, by
204 using a non-linear, least squares optimisation to solve equations (4) and (5), to determine initial
205 concentrations of Mn(II) and Mn(III) (Mn_0(II) and Mn_0(III), respectively). The sum of these
206 concentrations gives the total dissolved Mn concentration within the sample.

$$Mn^{3+}\cdot\text{T(4-CP)P}_{from\ Mn^{2+}_{aq}} = Mn_0^{2+}\left(1 - e^{-k_1 t}\right) \quad (4)$$

$$Mn^{3+}\cdot\text{T(4-CP)P}_{from\ Mn^{3+}_{aq}} = Mn_0^{3+}\left(1 - e^{-k_2 t}\right) \quad (5)$$

207

208 *(Where 'k_1' and 'k_2' are the rates of complex formation from* Mn(II) *and* Mn(III) *respectively)*

209 A Cary 50 UV-vis spectrophotometer was used to analyse the water samples using this kinetic
210 method, with the Mn(III)–T(4-CP)P complex being measured at its peak absorbance wavelength
211 (468 nm) in a 1cm pathlength quartz cuvette. For each kinetic scan, the cuvette was filled with
212 the following (in order):

213 • 2100 μL DI water

214 • 120 μL Buffer solution

215 • 80 µL $CdCl_2$ solution

216 • 400 µL T-(4-CP)P solution *(a greater volume than reported in Luther et al. (2015) was used as*
217 *this yielded more consistent results in this investigation. We considered that a greater*
218 *concentration of porphyrin was needed to outcompete the concentrated ambient ligand*
219 *concentration in the WTW)*

220 Following initiation of the scan at 2 s, a brief base-absorbance value was taken with the T-(4-
221 CP)P solution. After 10 s the scan was paused, 300 µL of the filtered sample (or standard) was
222 added to the cuvette, mixed using a pipette, and the scan restarted (within a target timeframe of 6
223 s). The scan was then allowed to run for up to 900 s, although it was generally stopped once the
224 absorbance readings had fully plateaued, typically after 200 s. The difference in results occurring
225 from removing the cuvette to shake the solution (based on Madison et al., 2011 and Luther et al.,
226 2015) for mixing and mixing in-situ using the pipette was found to be negligible, hence the more
227 practical approach of in-situ mixing was adopted. The volume of sample used for the
228 measurements depended on the concentration of Mn and varied between 1200 µL and 75 µL. As
229 the sample volume was varied, the volume of DI water added was adjusted accordingly to
230 maintain a total volume of 3 mL. The dilution relative to the original volume of 300 µL was
231 accounted for in the final calculation. Mn(II) standard solutions were analysed to produce a value
232 for 'k_1', which was found to be an order of magnitude lower than that presented in other work
233 (Madison et al. 2011, Luther et al. 2015). As a result, the k values used in this project were
234 calculated separately for each individual analysis, based on the 'k_1' values found experimentally,
235 and constraints defined in Luther et al. (2015).

236 ***2.3.1.2 Processing of Kinetic Scan Data***

237 The absorbance-time data produced by each kinetic scan were analysed in a customised Excel
238 spreadsheet, where the first meaningful data point — after addition of the sample to the cuvette
239 — in the scan data could be trimmed to the origin to allow proper determination of the rates of
240 complexation of the Mn(II) and Mn(III). This was critical to enable precise determination of the
241 concentrations of the Mn species present. This curve-trimming and fitting is shown as Figure S1
242 the Supplementary Material.

243 The inbuilt Excel SOLVER function was used to minimise the χ^2 value (between the laboratory
244 kinetic data and the values calculated from the optimised equations), by changing certain values
245 within prescribed constraints. Firstly, the sum of the concentrations of Mn(II) and Mn(III) was
246 set to be within 10% of the total dissolved Mn concentration of the sample, as determined using
247 the absorbance of the solution at the end of the scan and the Beer-Lambert Law. Secondly, 'k_1'
248 (see Eqn 4) was constrained to be within 2σ of the mean value of 'k_1' calculated in the
249 laboratory. Thirdly, 'k_2' (see Eqn 5) was constrained to be an order of magnitude less than 'k_1'
250 (as noted by Madison et al (2011)).

251 The mean k-values (and ranges) determined for each location are presented in Table 2 in Section
252 3.2.

253 ***2.3.2 Determination of Mn oxide***

254 Influent water was tested for the presence of Mn oxide colourimetrically using 0.04%
255 leucoberbelin blue (LBB, Sigma–Aldrich, UK) in 0.45 mM acetic acid since the colourless LBB
256 reagent changes to blue via oxidation with Mn(IV) when present (Krumbein and Altmann 1973).
257 Initally samples of concentrated unfiltered raw influent water were checked for reactivity with
258 LBB. As LBB also reacts with Mn(III), influent water was passed through a 0.2 μm filter and the

filtrate (<0.2 μM, dissolved fraction) and filtered particulate fraction (>0.2 μm) tested. A few drops of the 0.04 % LBB reagent were added to the samples and the presence of MnO_2 was confirmed when a blue colour change was observed.

2.4 Analytical methods

Atomic Force Microscopy (AFM) and Transmission Electron Microscopy Energy Dispersive Spectroscopy (TEM - EDS) were used to characterise samples of the water, both as-collected and concentrated by ultrafiltration. Concentration was carried out in a 400 mL Amicon stirred ultrafiltration unit with a 10 kDa ultrafiltration membrane at 20 psi nitrogen pressure. The water volume was reduced to approximately 1/40 of the original volume with the water and dissolved ions removed and nanoparticles concentrated in the water above the membrane.

2.4.1 AFM

Freshly cleaved mica sheets (Agar Scientific) were cut to produce 7×7 mm substrates. 50 μL of the concentrated raw water sample was deposited onto the mica sheets. The samples were covered for one hr and then residual liquid was wicked away with a tissue. The mica substrates were washed 4 times by immersion in 25 mL aliquots of ultrapure water for 30 s, to remove any residual salts, and air-dried overnight at room temperature under a dessicator lid to stop air-borne particles falling on the samples.

Sizes and shapes of the nanoparticles were obtained by AFM using a XE100 instrument (Park Systems). The samples were analysed in non-contact mode using a Si cantilever (PPP-NCHR, Park Systems). Images covering and area of 10 x10 μm were acquired, and heights of particles were measured using the XEI software (Park Systems).

2.4.2 TEM-EDS

30 µL of the sample was deposited onto carbon film on 200 mesh copper grids (Agar Scientific). The samples were covered for 1 hr, then the residual liquid was removed. The grids were washed four times, by immersion in 25 mL aliquots of ultrapure water for 30 s, and dried overnight.

Sizes and shapes of nanoparticles and aggregates were characterised on a JEOL1200EX transmission electron microscope (TEM), using 80 keV electron generation. The chemical compositions of nanoparticles were determined by Energy-Dispersive X-ray Spectroscopy (EDS) in a Jeol 2100 TEM, using 200 keV electron generation.

3.0 Results and Discussion

3.1 Influent water

Table 1 shows the variation in chemistry of pH, TOC, turbidity, dissolved Fe, dissolved Mn, alkalinity and hardness for the influent raw water as well as temperature and rainfall. There were no discernible trends between any of these parameters.

Figure 3 shows the raw influent water to the WTW contains two size fractions of particles, one which is 300-500 nm in size and one which is 50 nm in size. These have been identified using TEM and EDS as firstly clay particles and secondly humic substrances. Both the large clay particles and the smaller humic particles have Fe oxide precipitates (detected by EDS) on their surfaces (see Figure 4). Manganese is not detected and since it is present at $1/5^{th}$ the concentration of the Fe (see Table 1) it is likely to be below the detection rate for TEM/EDS.

304 It is known that manganese can occur in peaty soil pore waters as nano-particulate Mn oxides
305 around 1-3 nm (Krachler et al. 2012). The presence of Mn oxides in the raw influent peaty water
306 was confirmed using the LBB test (Supplementary Material Figures S2 and S3). The raw influent
307 water and particulate fraction (>0.2 μm) reacted positively with the LBB reagent showing a
308 strong blue colouration (see Supplementary Material, Figure S2b). The filtrate (<0.2 μm), where
309 Mn(III) is present, did not react with the LBB (Supplementary Material, Figure S2c) therefore
310 we conclude that the LBB reacted with Mn oxides which are present in the raw influent water as
311 particulates (although not nanoparticulate like Krachler et al. (2012) found) and that the
312 dissolved Mn(III) in the form present in this study does not react with the reagent. It is assumed
313 that the solid Mn oxide phase identified in the raw influent water is associated with the iron
314 oxide phase identified by TEM in Figure 4. It is interesting to note that in Figure 4 the form of Fe
315 oxide precipitation is linear and appears to follow a linear 'railway track' pattern. This linear
316 pattern is seen in the Fe oxide precipitates on both the clay particles and humic substances which
317 suggest that a similar mechanism is contolling precipitation in each case.

318 **3.2 Mn flux and speciation throughout the WTW**

319 It was possible to positively identify Mn(III) at all stages of the WTW (see Table 2). Full
320 analysis of Mn(III) throughout the plant was not possible due to difficulties in applying the
321 method to the highly coloured and semi-solid ferric sulphate coagulant and to the WTR. For this
322 reason the % Mn results presented in Table 2 for the ferric sulphate and WTR were determined
323 from product specification data and historic plant data provided by the water company NWG
324 Ltd.

325 The method allows the separation of the final dissolved Mn concentration into separate

326 concentrations of each Mn species, from which the percentage of Mn(III) at each stage of the
327 WTW can be calculated. The historic NWG Ltd. data were used to produce a mean value of flow
328 rate and of Mn concentration (in mg/kg WTR) within the WTR, which could then be used to
329 calculate a daily mass of Mn passing through the WTW, using a mean value of daily sludge
330 production, again determined from historic NWG Ltd. data. The results clearly show a decrease
331 in total Mn through the stages of the principal water treatment stream, with the majority of the
332 Mn being removed in the clarifiers and RGFs (see Table 2).

333 In the waste stream there are notably higher Mn concentrations, with the thickened and mixed
334 sludge having mean concentrations 160× greater than those found in the raw water entering the
335 plant (Table 2).

336 Besides the raw water input to the system (see Figure 5a), there are several stages which act to
337 introduce additional Mn throughout the system (see also Figures S4-S8 in Supplementary
338 Material). The supernatant (see Figure 5b) and backwash water is returned to the head of the
339 works to be mixed with the incoming raw water in the flash mixers (see Figure 1), hence adding
340 water with a significantly elevated concentration of previously removed Mn back into the
341 system. The addition of ferric sulphate as a coagulant to the clarifiers also introduces a new
342 source of Mn to the system (full removal of Mn during manufacture of Fe sulphate would
343 decrease the Fe content of the product). The relative quantity of Mn added as part of the ferric
344 sulphate addition can be seen in Table 2.

345 Figure 5b shows that of Mn(III) is higher when water is in contact with NOM which is present in
346 the sludge tanks (see stage 6 in Figure 1).

347 **3.3 Significance of Mn(III) identification in WTW**

Figure 5 shows that dissolved Mn(III) in solution is present in the raw water entering the WTW, but it is highly variable with a range of percentage total Mn from 0 to 100 %. We hypothesise that this Mn(III) has been formed by reductive dissolution of particulate Mn oxides (identified by the LBB test and associated with the iron oxides identified in Figure 4) by humic substances (also identified in Figure 4). In addition to the Mn(III) present in the influent raw water Mn(III) was found in all of the seven stages of the WTW (see Table 2). The addition of lime through the process raises the pH of the water, making it easier for dissolved Mn to precipitate out of solution as an oxide (Tebo et al. 2004), and decreasing the total quantity of dissolved Mn present in solution. Madison et al. (2011) and Trouwborst et al. (2006) suggest that Mn(III) is more likely to remain in solution if it is complexed with strong organic ligands. Therefore, it is likely that the Mn(III) which is still present in the water at the later stages of the principal treatment process is more strongly bound to organic ligands in the water, and hence resists removal via oxidation.

The concentrations of Mn(III) within the principal water treatment stream were found to be much lower (by one or two orders of magnitude respectively) than those detected by Trouwborst et al. (2006) and Madison et al. (2011) both of which studied suboxic environments. However, with the exception of the sludges, the WTW environment is, by design, oxic in nature, hence Mn(III) is far more likely to be oxidised to solid MnO_2 and thus be removed from solution. However, the solid waste stream water within the plant contains an extremely high proportion of Mn(III), with values of up to 70% in some samples, and a mean value of 49 % in the samples of mixed and thickened sludge (Table 2).

The concentrations of Mn(III) found in the mixed & thickened sludges (stage 6 in Figure 1) had a mean of 1078 µg/L. Given the significantly concentrated nature of the sludges which contain

371 significant NOM this is not unexpected. These sludges sit in settlement tanks for several days,
372 and are likely to be at least partly suboxic in nature, similar to the environments studied by
373 Trouwborst et al. (2006), Madison et al. (2011) and Oldham et al. (2017). The Mn(III)
374 concentrations in the mixed and thickened sludges were higher than those found in the suboxic
375 zones of the Black Sea (up to 275 μg/L) (Trouwborst et al. 2006) but lower than the Mn(III)
376 concentrations determined in suboxic sediment porewaters in the lower St Lawrence Estuary (in
377 excess of 3300 μg/L in the organic matter decomposition zone) (Oldham et al. 2017).

378 The concentrations of Mn(III) found in the clarifier sludges (stage 5 in Figure 1) were lower, at
379 144 μg/L, and comparable to the range found within the suboxic waters of the Black Sea
380 (Trouwborst et al. 2006). This is perhaps to be expected given the less-concentrated nature of the
381 clarifier sludges in comparison to the mixed and thickened sludges. The Mn-oxides found in the
382 RGFs are passed, via the backwash water, to the sludge settlement tanks allowing for mixing
383 between Mn oxides and natural organic matter. These provide reducing conditions which may
384 favour the reduction of Mn oxides to Mn(III) species. Mn(III) is therefore being produced and
385 likely stabilised within the sludge tanks of the WTW. The concentration of dissolved Mn within
386 the wash water and supernatant recycling stream is greatly diminished compared to that which is
387 present in the solid waste stream; however it is still greatly in excess (approximately 15×) of that
388 of the raw water inflow to the plant (6.7 μg/L – see Table 2).

389 Trouwborst et al. (2006) state that unknown organic ligands are responsible for stabilising
390 Mn(III) in natural waters. The increased Mn(III) concentration in locations of elevated organic
391 matter (such as the raw water inflow, clarifiers, sludges and supernatant and backwash flows)
392 throughout the treatment process, corroborates the idea of an organic ligand stabilising the
393 Mn(III) in solution.

394 This investigation does not explore what this or these organic ligands are, but it is clear that dark
395 humic substances are present in both the solid and liquid waste streams (Figure 6).

396 The principal source of humic substances is the peat uplands where the water originates before
397 transferring to Derwent reservoir. Johnson et al. (2015) have studied the stabilisation of this
398 dissolved organic carbon in the Mn oxide layers around the sand grains used as the filter media
399 in the RGF at the Mosswood WTW in NE England. They postulate that the significant stability
400 of the carbon, including under thermal duress, results from the carboxylate groups within the
401 organic carbon bonding with the Mn oxide surface, as well as the physical entrapment of the
402 carbon within the layers of the Mn oxide mineral birnessite. The role of Mn(III) in this system
403 was not explored for this study but it is clear that Mn removal via Mn oxide precipitation
404 (Johnson et al 2015) and WTR production in WTW (Finlay et al 2016) plays an important but
405 overlooked role in trapping carbon.

406 Environmental data, including historic NWG Ltd. WTW data of influent raw water content and
407 UK Meteorological Office weather data (rainfall and temperature) (see Table 1), were studied to
408 determine whether there were any significant trends between the concentration of dissolved Mn
409 in the influent and other environmental and temporal factors. It is hypothesised that influent
410 dissolved organic carbon [DOC ~10 mg/L, (Johnson et al. 2015)] is reducing influent particulate
411 Mn oxides to produce dissolved Mn(III)-organic ligands. Under oxic conditions it is assumed
412 that there is no MnO_2 reduction by the direct microbial anaerobic respiratory process (Nealson
413 and Saffarini, 1994). No significant trends or correlations were identified over the 2 month
414 sampling period between meteorological factors or other chemical parameters presented in Table
415 1 (e.g. TOC and dissolved Mn). In contrast, other studies have found a link between the
416 concentration of dissolved Mn and DOC in similar upland soil waters (Hardie et al., 2007). The

lack of correlation between Mn and TOC in our data may be due to the fact that the influent raw water is coming from a reservoir which may have obscured any correlations.

Another source of organic ligands could be through contamination of reagents added to the treatment process. It is plausible that some component of humic substances could survive industrial processing, and hence be introduced to the plant through contaminated reagents such as the ferric sulphate coagulant. It is also possible that there is Mn(III) present in the ferric sulphate as a component of the naturally occurring Mn, and that this Mn(III) is stabilised by strong organic ligands which have not been removed in the manufacturing process.

4.0 Conclusions

Both Mn oxides and Mn(III) have been detected in the influent raw peaty water of the WTW. It is hypothesised that Mn oxides are reduced by DOC or NOM in the influent water to make Mn(III) organic ligands. Mn(III) is positively identified at every stage throughout the WTW. The waste water streams have the highest proportions of Mn(III) with 49 % (range 17 – 89 %) of the total dissolved Mn was present as Mn(III) in the mixed and thickened clarifier sludge supernatant (which contained a mean of 1078 μg/L). Importantly this means that Mn(III) is produced within the WTW through interaction of Mn oxide solids with NOM in the sludges and concentrations are likely to be highest where this contact time is greatest. There is no evidence for preferential removal of either dissolved Mn(II) or Mn(III). However, if one is preferentially removed over the other, the ratio of Mn(II)/Mn(III) could potentially be manipulated within WTWs by increasing or decreasing the amount of time supernatant water was in contact with waste sludges. This may potentially provide benefits to the water industry by allowing them to move towards

optimising dissolved Mn removal and therefore reducing discoloration events in the network pipes.

Competing financial interests statement. The authors declare no competiting financial interests.

Acknowledgements

Funding for this work was provided by the Leverhulme Foundation (Philip Leverhulme Prize PLP-2011-111) and is gratefully acknowledged. We thank Northumbrian Water Group for all of their support in this work, and the two anonymous reviewers whose comments significantly improved the paper.

References

Bruins, J.H., Petrusevski, B., Slokar, Y.M., Huysman, K., Joris, K., Kruithof, J.C. and Kennedy, M.D. (2015) Biological and physico-chemical formation of Birnessite during the ripening of manganese removal filters. Water Research 69 (Supplement C), 154-161. https://doi.org/10.1016/j.watres.2014.11.019

Davies, G., (1969) Some aspects of the chemistry of manganese(III) in aqueous solution. Coordination Chemistry Reviews 4, 199–224. https://doi.org/10.1016/S0010-8545(00)80086-7

458 Finlay, N.C., Johnson, K. & Worrall, F. (2016). The role of water treatment abstraction in the
459 flux and greenhouse gas emissions from organic carbon and nitrogen within UK rivers. Water
460 Resources Research52(10): 8190-8201.
461 https://doi-org.ezphost.dur.ac.uk/10.1002/2016WR019362
462
463 Hardie, A., Heal, K. and Lilly, A. (2007) The Influence of Pedology and Changes in Soil
464 Moisture Status on Manganese Release from Upland Catchments: Soil Core Laboratory
465 Experiments. Water, Air & Soil Pollution 182(1-4), 369-382. https://doi-
466 org.ezphost.dur.ac.uk/10.1007/s11270-007-9348-6
467
468 Hu, E., Zhang, Y., Wu, S., Wu, J., Liang, L. and He, F. (2017) Role of dissolved Mn(III) in
469 transformation of organic contaminants: Non-oxidative versus oxidative mechanisms. Water
470 Research 111(Supplement C), 234-243. https://doi.org/10.1016/j.watres.2017.01.013
471
472 Jiang, J., Pang, S.-Y., Ma, J. (2010). Role of Ligands in Permanganate Oxidation of Organics.
473 Environ. Sci. Technol. 44, 4270–4275. https://doi.org/10.1021/es100038d
474
475 Johnson, K., Purvis, G., Lopez-Capel, E., Peacock, C., Gray, N., Wagner, T., Marz, C., Bowen,
476 L., Ojeda, J., Finlay, N., Robertson, S., Worrall, F. and Greenwell, C. (2015) Towards a
477 mechanistic understanding of carbon stabilization in manganese oxides. Nat Commun 6. DOI:
478 10.1038/ncomms8628 | www.nature.com/naturecommunications
479

480 Johnston, R. (2011) Trunk Mains Cleaning Programme: Northumbrian Water's £30 million
481 project to clean and refurbish 157km of trunk mains in Tyneside and South East
482 Northumberland. www.waterprojectsonline.com/case_studies/2011/Northumbrian_Mains_2011.pdf
483
484 Krachler, R., Von Der Kammer, F., Jirsa, F., Süphandag, A., Krachler, R.F., Plessl, C., Vogt, M.,
485 Keppler, B.K. and Hofmann, T. (2012) Nanoscale lignin particles as sources of dissolved iron to
486 the ocean. Global Biogeochemical Cycles 26(3). doi:10.1029/2012GB004294, 2012
487
488 Krumbein, W.E. and Altmann, H.J. (1973) A new method for the detection and enumeration of
489 manganese oxidizing and reducing microorganisms. Helgoländer Wissenschaftliche
490 Meeresuntersuchungen 25(2-3), 347-356. https://link-springer-
491 com.ezphost.dur.ac.uk/content/pdf/10.1007%2FBF01611203.pdf
492
493 Luther, G.W., Madison, A.S., Mucci, A., Sundby, B. and Oldham, V.E. (2015) A kinetic
494 approach to assess the strengths of ligands bound to soluble Mn(III). Marine Chemistry
495 173(Supplement C), 93-99. https://doi.org/10.1016/j.marchem.2014.09.006
496
497 Madison, A.S., Tebo, B.M. and Luther, G.W. (2011) Simultaneous determination of soluble
498 manganese(III), manganese(II) and total manganese in natural (pore)waters. Talanta 84(2), 374-
499 381. https://doi.org/10.1016/j.talanta.2011.01.025
500
501 McCann, C.M., Gray, N.D., Tourney, J., Davenport, R.J., Wade, M., Finlay, N., Hudson-
502 Edwards, K.A. and Johnson, K.L. (2015) Remediation of a historically Pb contaminated soil

using a model natural Mn oxide waste. Chemosphere 138, 211-217. https://doi.org/10.1016/j.chemosphere.2015.05.054

Menezes-Filho, J.A., Bouchard, M., Sarcinelli Pde, N. and Moreira, J.C. (2009) Manganese exposure and the neuropsychological effect on children and adolescents: a review. Rev Panam Salud Publica 26(6), 541-548. https://scielosp.org/scielo.php?script=sci_arttext&pid=S1020-49892009001200010&lng=en&nrm=iso&tlng=en

Nealson, K.H. and D. Saffarini (1994). Iron and manganese in anerobic respiration: environmental significance, physiology, and regulation. Annual Review of Microbiology. 48: 311-343).

Oldham, V.E., Mucci, A., Tebo, B.M. and Luther, G.W., III (2017) Soluble Mn(III)–L complexes are abundant in oxygenated waters and stabilized by humic ligands. Geochimica et Cosmochimica Acta 199, 238-246. https://doi.org/10.1016/j.gca.2016.11.043

Oldham, V.E., Owings, S.M., Jones, M.R., Tebo, B.M. and Luther, G.W. (2015) Evidence for the presence of strong Mn(III)-binding ligands in the water column of the Chesapeake Bay. Marine Chemistry 171, 58-66. https://doi.org/10.1016/j.marchem.2015.02.008

Sun, B., Guan, X., Fang, J., Tratnyek, P.G., 2015. Activation of Manganese Oxidants with Bisulfite for Enhanced Oxidation of Organic Contaminants: The Involvement of Mn(III). Environ. Sci. Technol. 49, 12414–12421. https://doi.org/10.1021/acs.est.5b03111

Tebo, B.M., Bargar, J.R., Clement, B.G., Dick, G.J., Murray, K.J., Parker, D., Verity, R. and Webb, S.M. (2004) Biogenic manganese oxides: Properties and mechanisms of formation. The Annual Review of Earth and Planetary Sciences 32, 287-328.

Trouwborst, R.E., Clement, B.G., Tebo, B.M., Glazer, B.T. and Luther Iii, G.W. (2006) Soluble Mn(III) in suboxic zones. Science 313(5795), 1955-1957. DOI: 10.1126/science.1132876

WHO (2011) Guidelines for drinking-water quality. Fourth edition, WHO, Geneva.

Yu, W., Campos, L., Shi, T., Li, G., Graham, N., 2015. Enhanced removal of manganese in organic-rich surface water by combined sodium hypochlorite and potassium permanganate during drinking water treatment. RSC Adv. 5, 27970–27977. https://doi.org/10.1039/C5RA01643F

Figure and Table captions

Figure 1: Schematic showing the processes and chemical additions within Mosswood Water Treatment Works, typical of many WTW which have provision for Mn removal. Numbers refer

551 to sampling locations used within this investigation. (1) Raw water (pH 7.4); (2) Clarifiers; (3)
552 Rapid Gravity Filters (RGFs) (pH 9.2); (4) Final Water Supply; (5) Clarifier Sludge Tank; (6)
553 Mixed & Thickened Sludge Tank; (7) Supernatant and Wash Water Return (pH 7.1)

554

555 **Figure 2:** Mn cycle in oxygenated systems showing relationship between dissolved Mn(II) in
556 solution, dissolved Mn(III) in solution as a Mn-C complex (where C represents a C-containing
557 ligand) and Mn(III) and Mn (IV) in solid Mn oxides.

558

559 **Figure 3:** Atomic Force Microscope image of concentrated influent raw water to the WTW
560 showing two lots of nanoparticles – larger clay particles 'flower-shaped' (300-500nm) with Fe
561 oxide precipitates (see Figure 4a) and smaller (30-50nm) humic substances 'snow-like' which
562 also have Fe oxide precipitates (see Figure 4b).

563 **Figure 4:** Transmission Electron Microscope image of nanoparticles in concentrated raw
564 influent water to WTW showing a) larger 300-500nm clay particles with Fe oxide (identified by
565 EDS) precipitates growing on clay surfaces and b) humic materials (50nm) with Fe oxide
566 precipitates growing on surface

567 **Figure 5:** Measured Mn (II) and Mn (III) in (a) raw water and (b) mixed and thickened sludge
568 for all samples analysed. Average Mn (III) in the raw water samples was 9 % [0- 100 %] and 49
569 % [17 – 89 %] in the sludge.

570

571 **Figure 6:** Photograph of typical samples from the solid and liquid waste streams (stages (5), (6)
572 and (7)), showing the relative proportions of suspended solids and supernatant after a settling

time in excess of 28 days. The thickened & mixed clarifier sludge sample (6) had solidified significantly and was difficult to disturb by shaking, whereas the other two samples were easily resuspended by shaking.

Table 1: Influent water chemistry for Mosswood WTW over a one-year period

Table 2: Mean Mn flux, speciation and k-values for each stage of the treatment process at Mosswood WTW. Values were determined over 12 identical sampling days with ranges presented in brackets.

Table

Click here to download Table: Table 1_WR42174R1.docx

Table 1: Influent water chemistry for Mosswood WTW over a one-year period

	Daily temperature (°C)	**Daily total rainfall (mm)**	**Dissolved Fe (ug/l)**	**Dissolved Mn (ug/l)**	**Total organic carbon (mg/l)**	**Alkalinity (mg/l HCO_3)**	**pH**	**Hardness (mg/l Ca)**	**Turbidity (NTU)**
Average	13.5	1.7	255.0	51.5	5.8	19.2	7.5	12.2	1.8
Min	0.7	0.0	180.0	23.0	5.4	13.0	7.3	11.0	0.9
Max	27.4	21.6	440.0	100.0	6.3	24.0	8.3	13.0	2.7
n	385	385	12	12	12	12	5	5	10

Table
Click here to download Table: Table 2_WR42174R1.docx

Table 2: *Mean Mn flux, speciation and k-values for each stage of the treatment process at Mosswood WTW. Values were determined over 12 identical sampling days with ranges presented in brackets.*

Location		Flow (ML/Day)	Dissolved Mn (µg/L)	Total Mn[1] (g/day)	Total Dissolved Mn (g/day)	Mn (II) (g/day)	Mn (III) (g/day)	Mn(III) (%)	K_1 s^{-1}	K_2 s^{-1}
Principal water treatment system	(1) Raw Water	139 [135-143]	4 [0-23]	7690	578 [0-3259]	566 [0-2575]	12 [0-684]	2 [0-21]	0.0471 [0.0293-0.0620]	0.028 [0.0019-0.052]
	(2) Clarifier Water		8 [0-23]	-	1067 [0-3344]	1003 [0-1873]	64 [0-1471]	6 [0-44]	0.0505 [0.0162 – 0.0620]	0.032 [0.0019-0.0076]
	(3) RGFs		4 [0-17]	-	623 [0-2408]	567 [0-409]	56 [0-1999]	9 [0-83]	0.0479 [0.0293-0.0620]	0.0024 [0.0019-0.0032]
	(4) Final Water		4 [0-15]	-	494 [0-2195]	469 [0-856]	25 [0-1339]	5 [0-61]	0.0402 [0.0293-0.0620]	0.0021 [0.0019-0.0032]
Waste stream	(5) Clarifier Sludge	1[2]	123 [13-215]	-	123 [13-215]	81 [12-75]	42 [2-140]	34 [12-65]	0.0567 [0.0383-0.0620]	0.0030 [0.0019-0.0101]
	(6) Mixed & Thickened Sludge	9[2]	919 [209-1558]	-	8274 [1879-14023]	5047 [1560-4067]	3227 [319-9956]	39 [17-71]	0.0566 [0.0401-0.0620]	0.0019 [0/0019-0.0019]
	(7) Supernatant & Wash Water Return	2[2]	73 [0-141]	-	146 [1-283]	120 [1-173]	26 [0-110]	18 [0-39]	0.0573 [0.0293-0.0620]	0.0019 [0.0019-0.0021]
	Ferric Sulphate	0.0043[3]	-	2700[3]	-	-	-	-	-	-
	WTR		-	52410[2]	-	-	-	-	-	-

[1] Total (i.e. particulate and dissolved) data for Mn was only available for the raw water, ferric sulphate and WTR.
[2] Personal communication from NWG Ltd., values are a typical percentages or concentrations and no ranges are presented.
[3] Taken from manufacturers information and also personal communication from NWG Ltd. No ranges are presented

Figure

Click here to download high resolution image

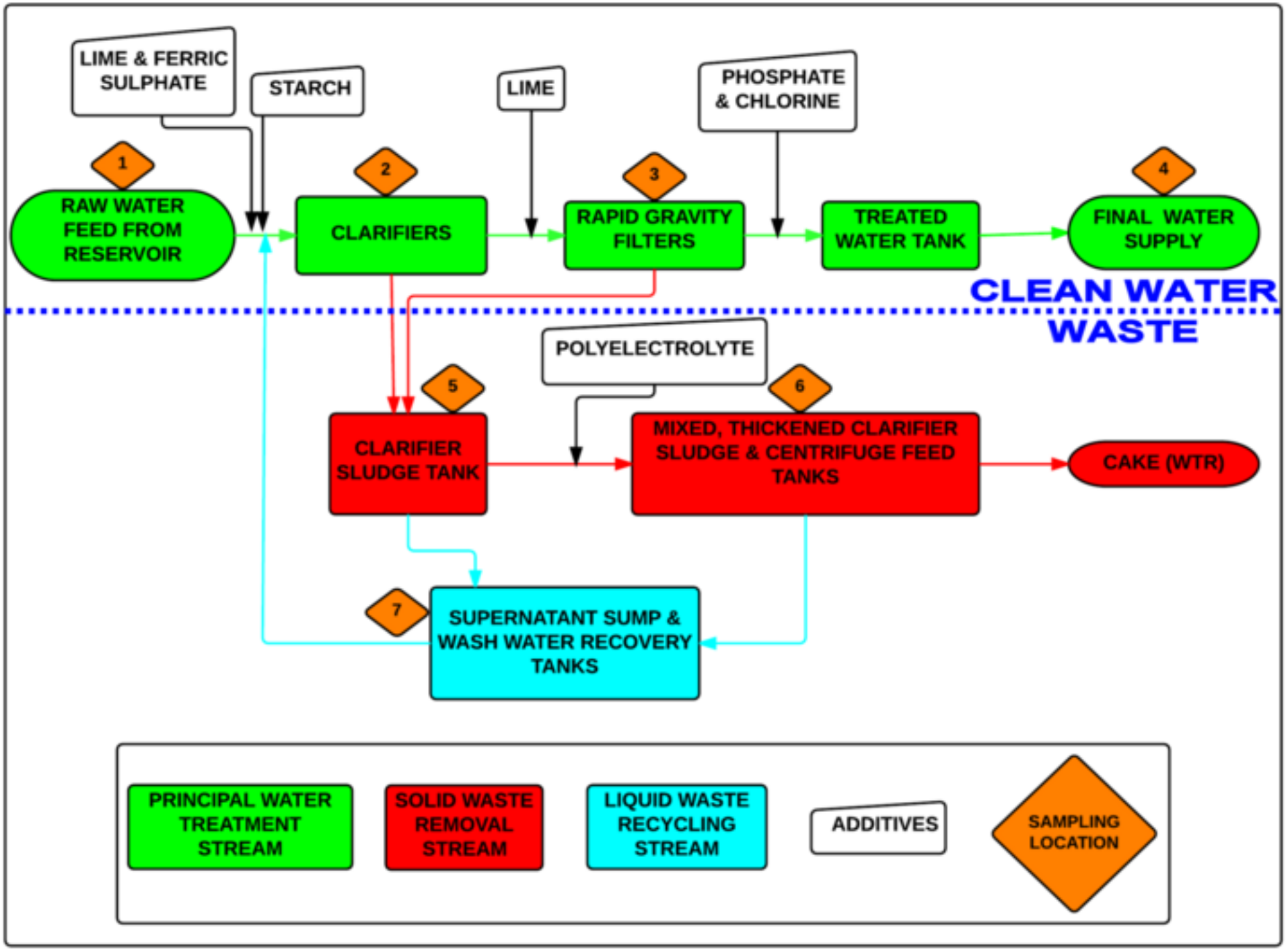

Figure

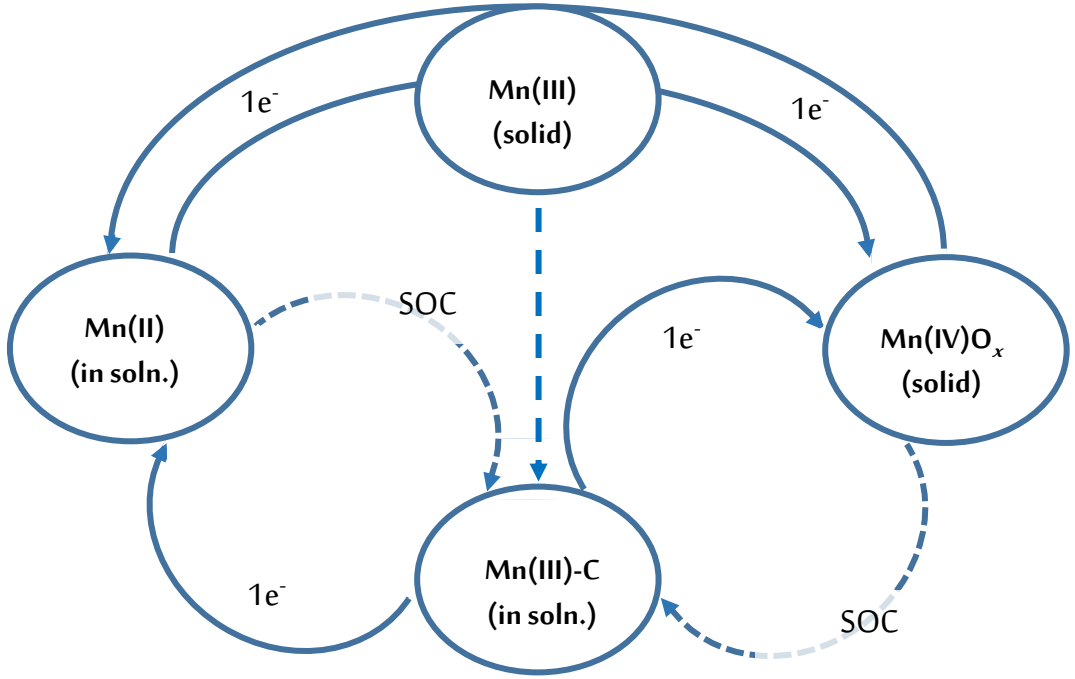
Mn(III)
(solid)
1e-
1e-
Mn(II)
(in soln.)
SOC
1e-
Mn(IV)Ox
(solid)
1e-
Mn(III)-C
(in soln.)
SOC

Figure

Click here to download high resolution image

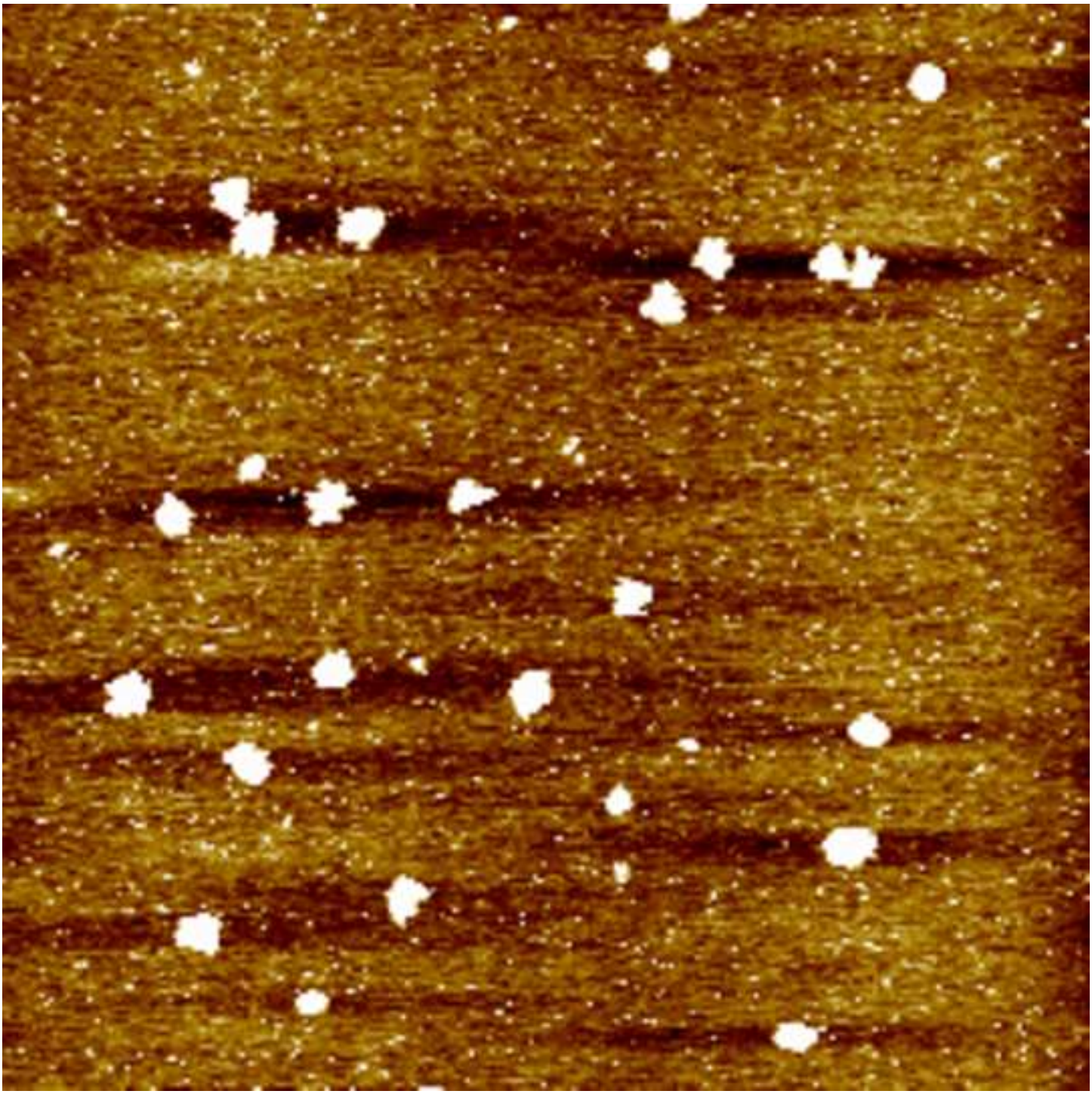

Figure

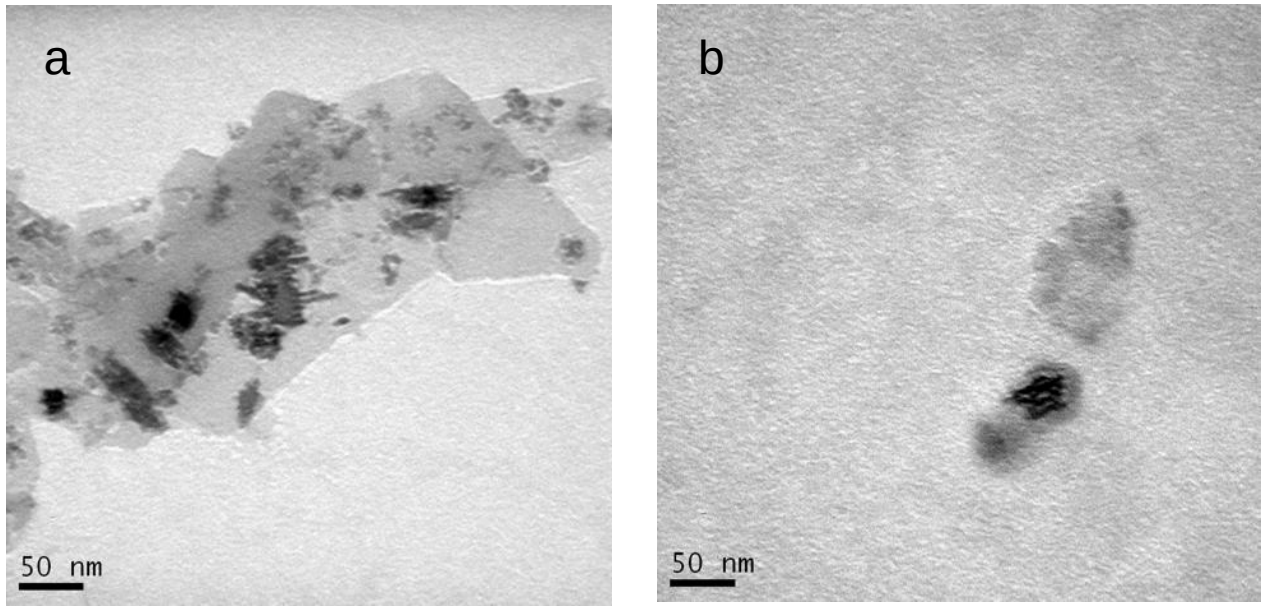

Figure

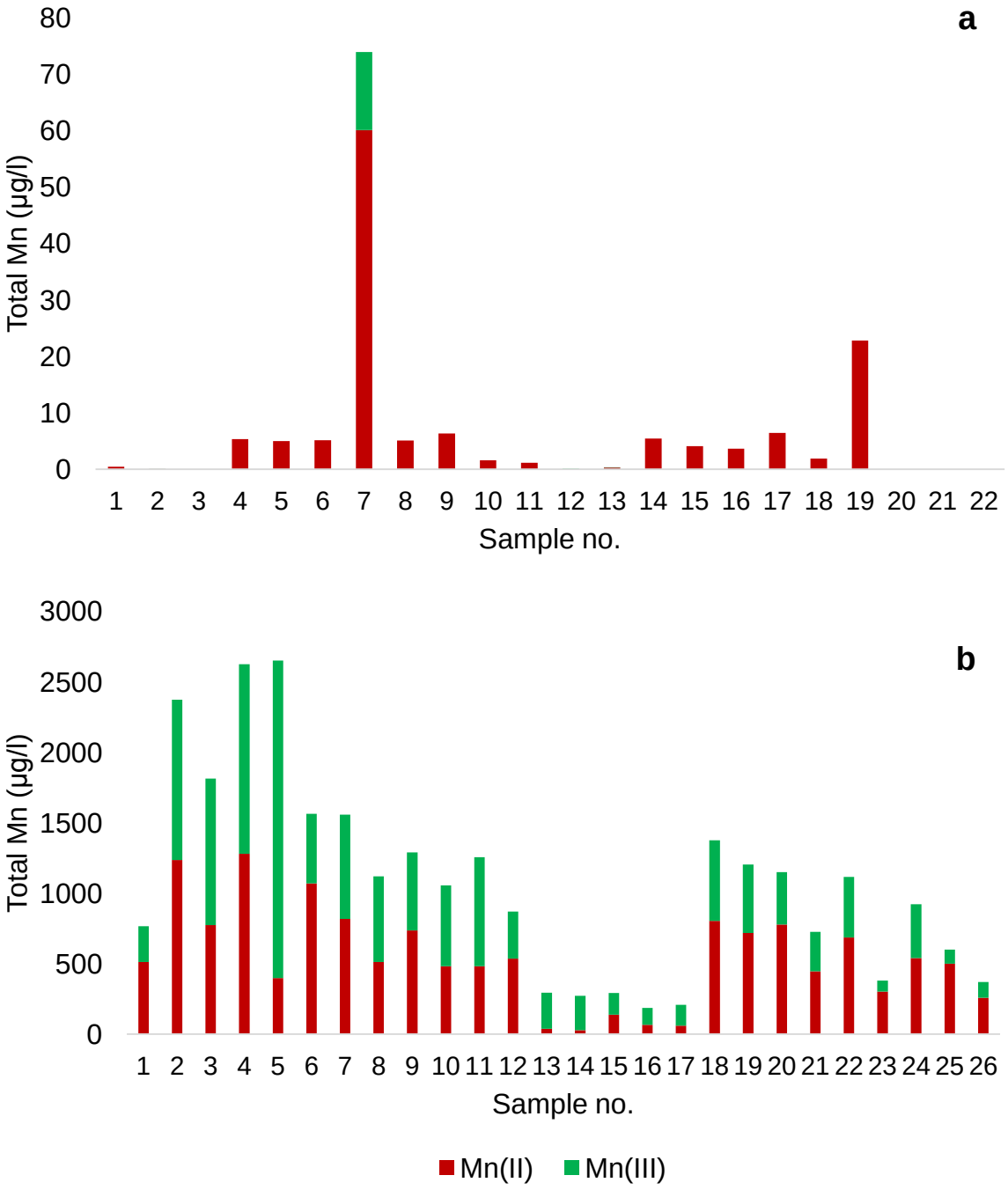

Figure 5. Measured Mn (II) and Mn (III) in (a) raw water and (b) mixed and thickened sludge for all samples analyzed. Average Mn (III) in the raw water samples was 9 % [0- 100 %] and 49 % [17 – 89 %] in the sludge.

Figure

Click here to download high resolution image

Dissolved Mn(III) in Water Treatment Works: Prevalence and Significance

Supplementary Material

Karen L. Johnson[1*], Clare M. McCann[2], John-Luke Wilkinson[3], Matt Jones[4&5], Bradley M. Tebo[5], Martin West[6], Christine Elgy[7], Catherine E. Clarke[8] Claire Gowdy[9] and Karen A. Hudson-Edwards[10]

[1]School of Engineering and Computing Sciences, Durham University, South Road, DH1 3LE

[2]School of Natural and Environmental Sciences, Newcastle University, Newcastle upon Tyne, NE1 7RU.

[3]AECOM, Newcastle upon Tyne, NE1 2HF.

[4] School of Environmental Science and Engineering, Pohang University of Science and Technology (POSTECH), 77 Cheongam-ro, Nam-gu, Pohang-si, Gyeoungsangbuk-do, 37673, Korea.

[5]Institute of Environmental Health, Oregon Health & Science University, Portland, OR 97239 USA

[6]School of Geography, Durham University, South Road, DH1.

[7]Facility of Environmental Nanoscience Analysis and Characterisation, Department of Geography Earth and Enviromental Sciences, Edgbaston, Birmingham, B15 2TT.

[8] Department of Soil Science, Stellenbosch University, Private Bag X1, Matieland 7602, South Africa.

[9]Northumbrian Water, Boldon House, Wheatlands Way, Pity Me, Durham, DH1 5FA

[10]Environment & Sustainability Institute and Camborne School of Mines, University of Exeter, Penryn, Cornwall, TR10 9DF

*Corresponding author: Karen Johnson (karen.johnson@durham.ac.uk)

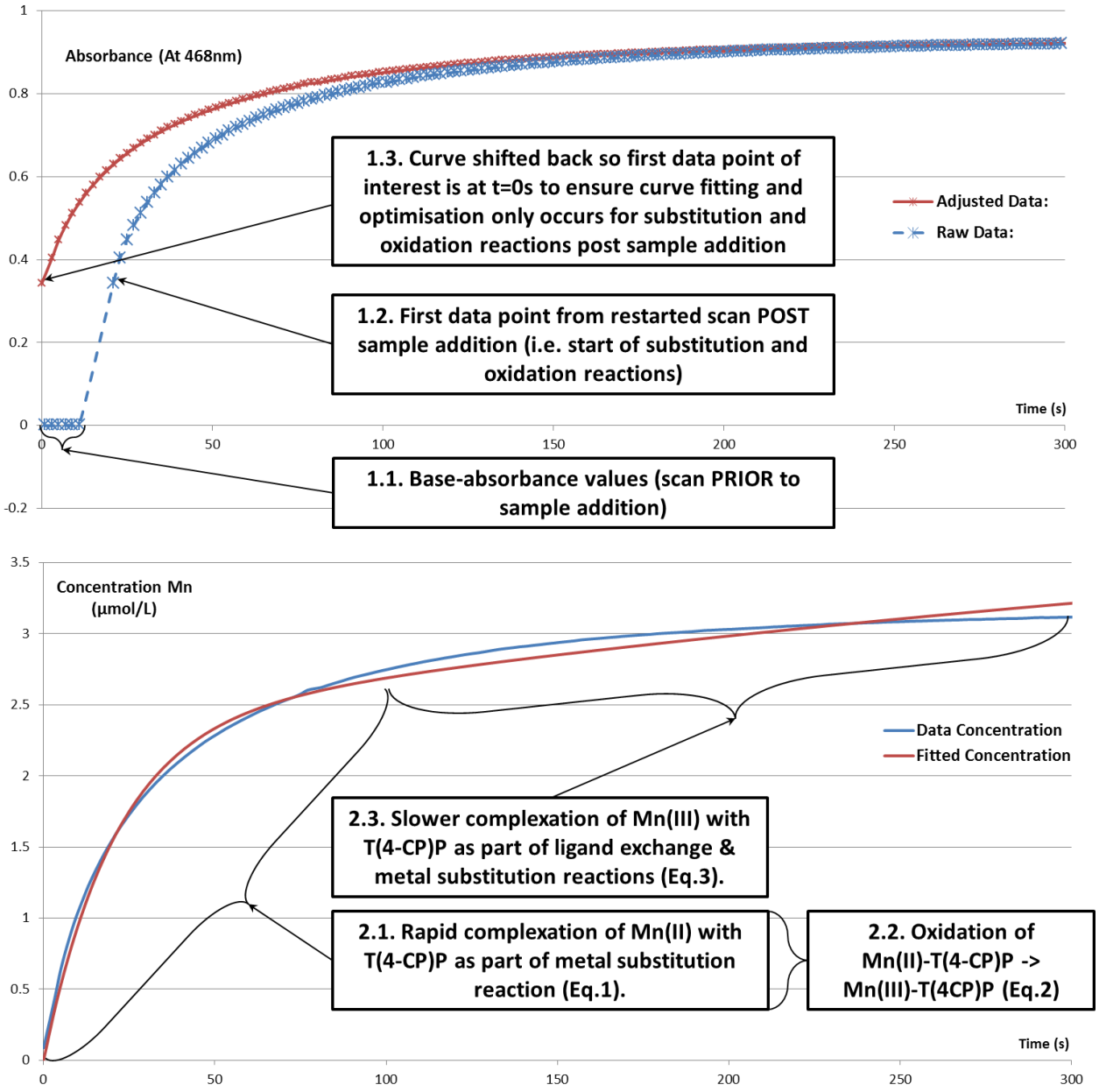

Figure S1: Top: Absorbance-Time kinetic scan data. The original (Spectrophotometer output data) are shown in blue, the modified data in red. Bottom: Total Dissolved Mn Concentration-Time Graph, showing curve fitting. Concentration of dissolved Mn = Concn of Mn(II) + Concn of Mn(III) (i.e., the sum of equations (4) & (5)). Concentration, calculated from the trimmed original data is shown as a blue line, and the data generated by the optimized curve fitting as a red line. (Both sets of curves generated for a sample of clarifier sludge).

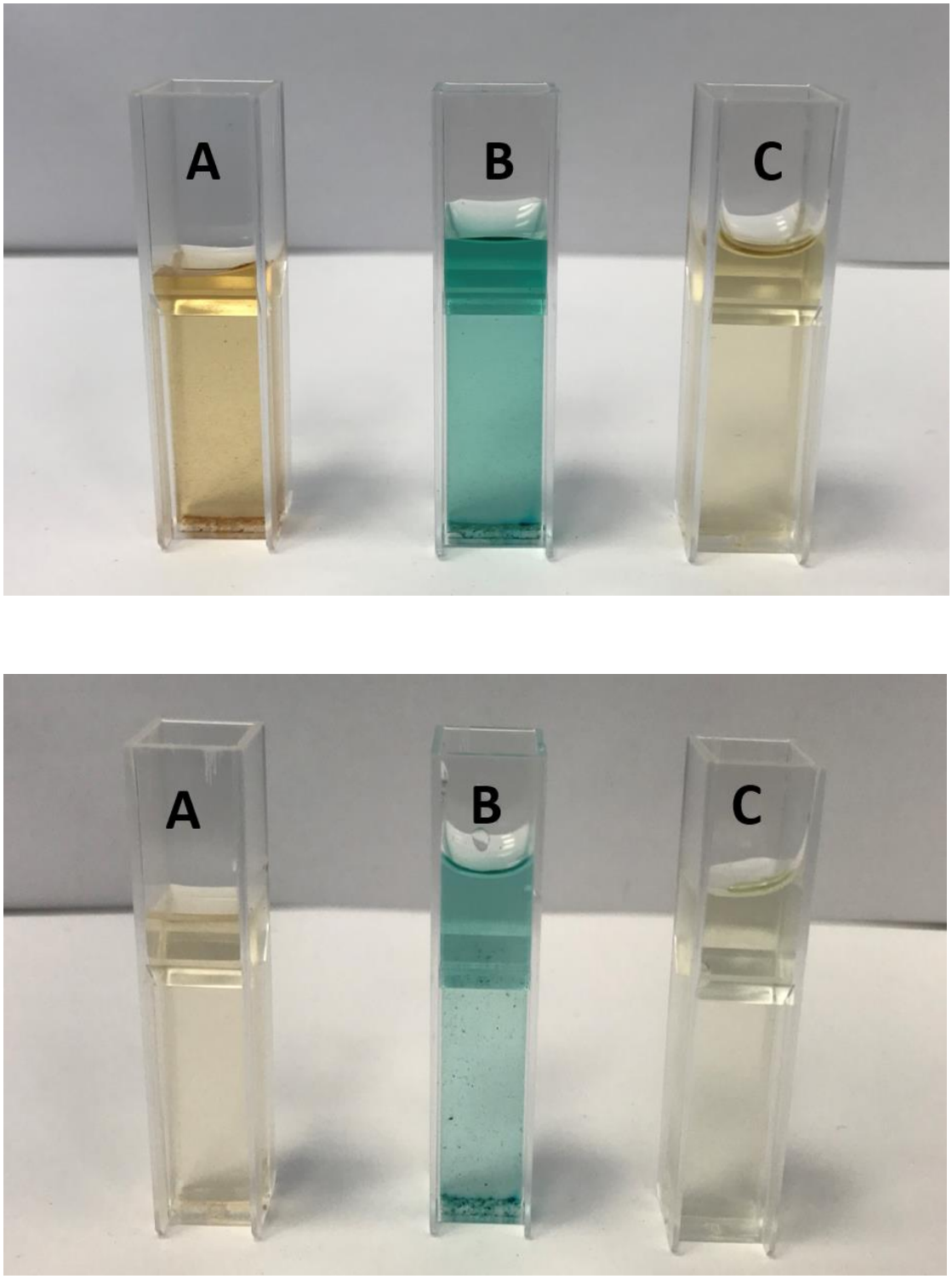

Figure S2: Pictures showing the testing for the presence of Mn oxides using LBB in influent water from Day 2 (top) and Day 3 (bottom); (a) influent water not filtered no LBB, (b) influent water not filtered with LBB, (c) 0.2 µm filtered water with LBB. Mn oxide is present in the influent water as shown form the blue colouration in (b), when filtered no Mn oxide is present due to no blue colouration (c).

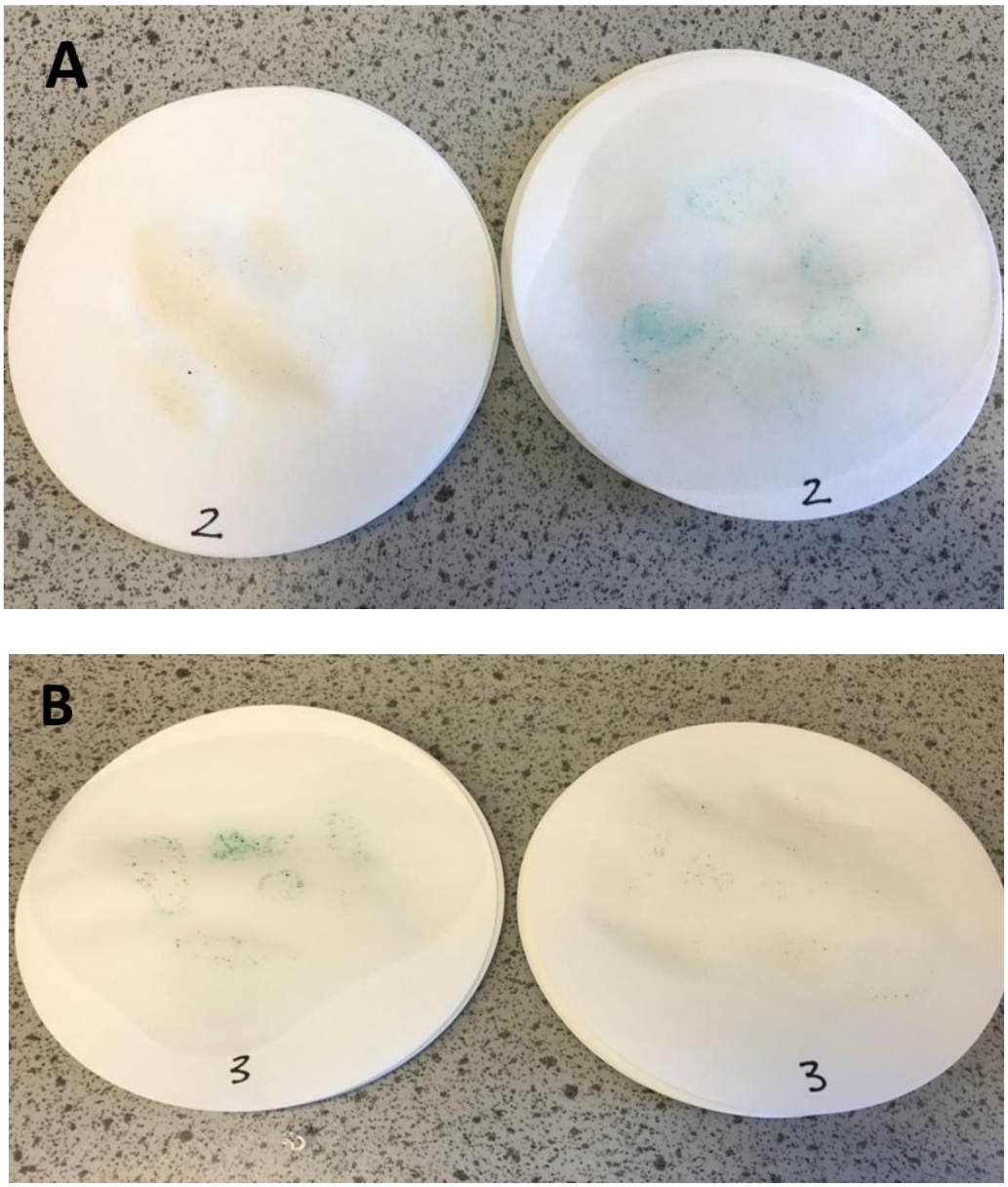

Figure S3: Pictures showing the testing for the presence of Mn oxides using LBB on filtered water > 0.2µm (a) sample from day 2 without LBB (left) with LBB (right) (b) sample from day 3 with LBB (left) without LBB (right). Mn oxide is present in the solids of the influent water, after filtration through paper you can see the blue colouration around particles left which is indicative of Mn oxide.

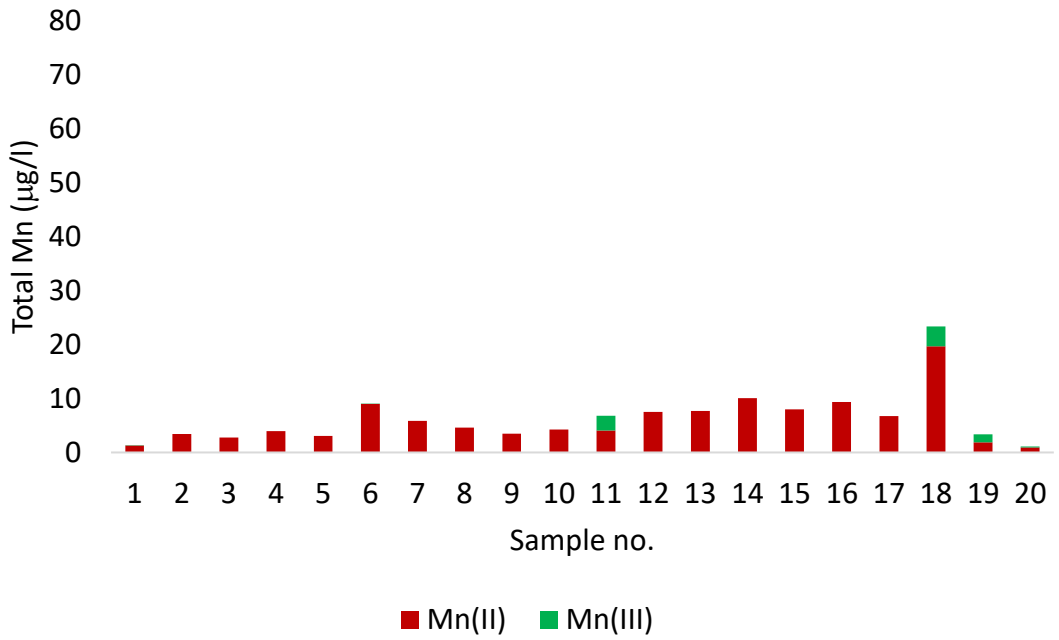

Figure S4: Measured Mn (II) and Mn (III) in the clarifier waters for all samples analyzed. Average Mn (III) in the samples was 6 % ranging from 0 - 44 %. Y-axis has been set to match the raw water data presented in Figure 5a in the manuscript for comparison.

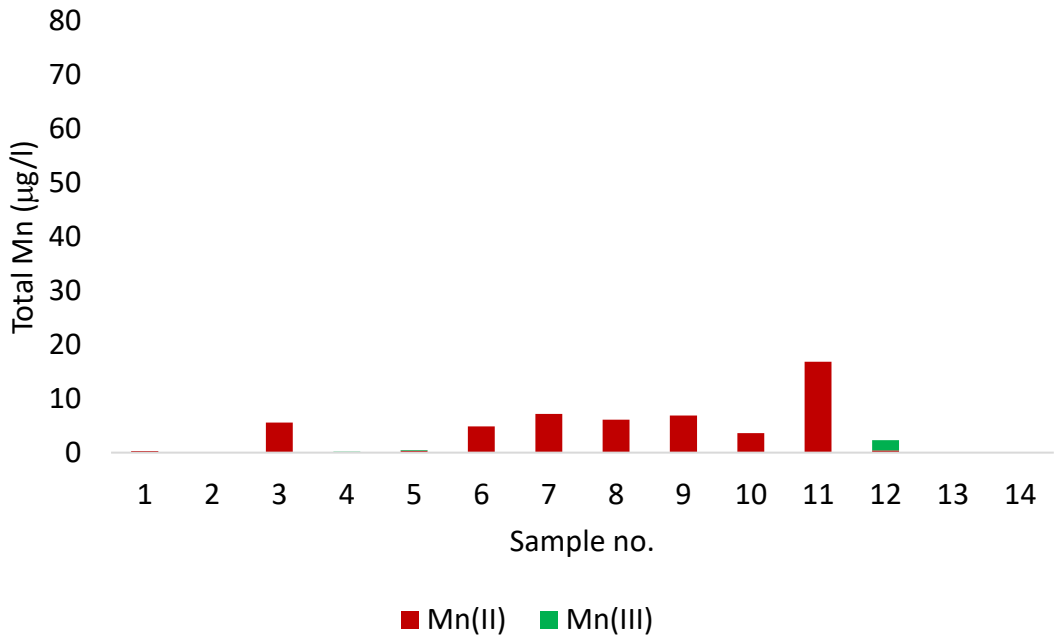

Figure S5: Measured Mn (II) and Mn (III) in the RGFs for all samples analyzed. Average Mn (III) in the samples was 13 % ranging from 0 - 83 %. Y-axis has been set to match the raw water data presented in Figure 5a in the manuscript for comparison.

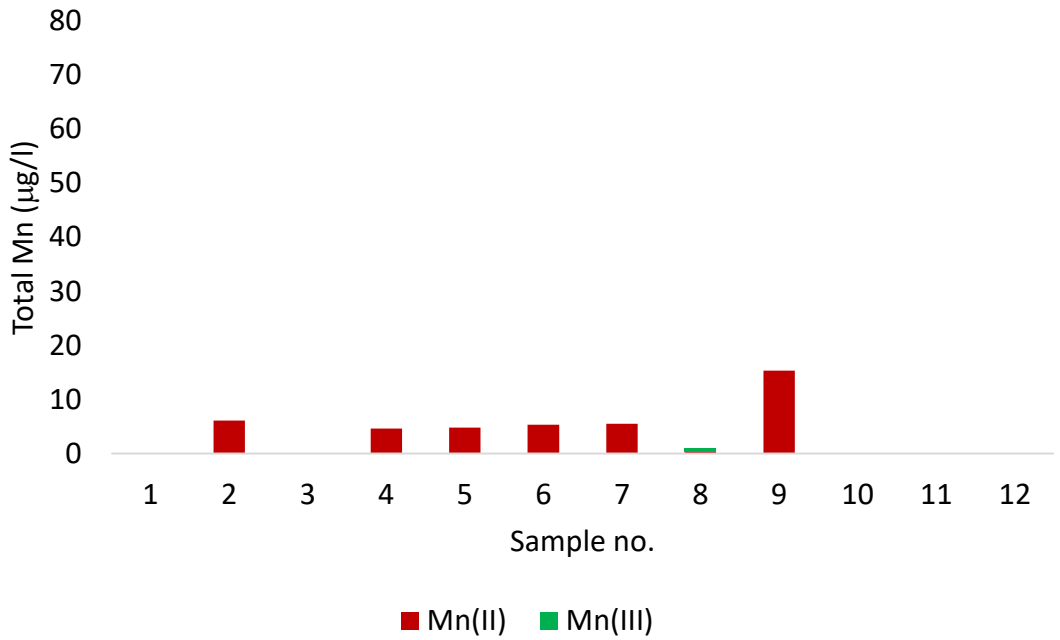

Figure S6: Measured Mn (II) and Mn (III) in the final water for all samples analyzed. Average Mn (III) in the samples was 9 % ranging from 0 - 61 %. Y-axis has been set to match the raw water data presented in Figure 5a in the manuscript for comparison.

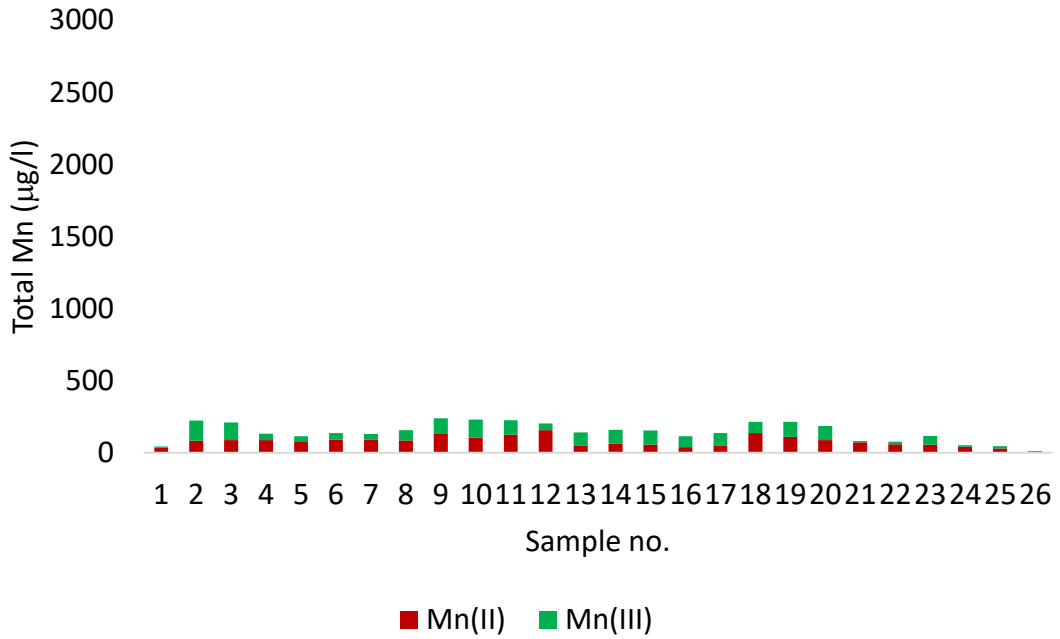

Figure S7: Measured Mn (II) and Mn (III) in the clarifier sludge for all samples analyzed. Average Mn (III) in the samples was 42 % ranging from 12 - 66 %. Y-axis has been set to match the mixed and thickened sludge data presented in Figure 5b in the manuscript for comparison.

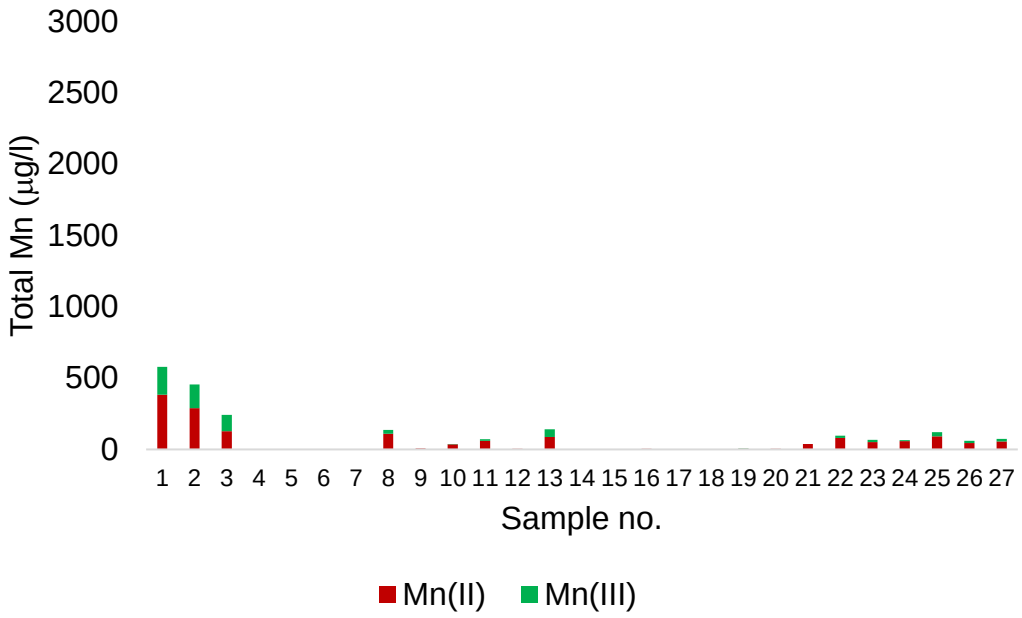

Figure S7: Measured Mn (II) and Mn (III) in the supernatant and water wash for all samples analyzed. Average Mn (III) in the samples was 14 % ranging from 0 - 47 %. Y-axis has been set to match the mixed and thickened sludge data presented in Figure 5b in the manuscript for comparison.